UC Irvine

UC Irvine Electronic Theses and Dissertations

Title

JAVELIN analysis of reverberation mapping data from the Lick AGN Monitoring Project 2011

Permalink

https://escholarship.org/uc/item/55q0m9zs

Author

Brandel, Andrew Peter

Publication Date

2017

Peer reviewed|Thesis/dissertation

eScholarship.org Powered by the California Digital Library
University of California

UNIVERSITY OF CALIFORNIA,
IRVINE

JAVELIN analysis of reverberation mapping data from the Lick AGN Monitoring Project 2011

THESIS

submitted in partial satisfaction of the requirements
for the degree of

MASTER OF SCIENCE

in Physics

by

Andrew Peter Brandel

Thesis Committee:
Professor Aaron Barth
Professor David Buote
Associate Professor Michael Cooper

2017

© 2017 Andrew Peter Brandel

TABLE OF CONTENTS

LIST OF FIGURES

LIST OF TABLES

ACKNOWLEDGMENTS

I would like to thank my committee chair and graduate advisor, Professor Aaron Barth for his support throughout my research. He helped me understand why my research was important and would always have literature for me to read on the topic instead of only answering the question in simple terms.

I would also like to thank Liuyi Pei for helping me understand how JAVELIN works and how to use it. She explained why JAVELIN would sometimes give an error and gave helpful suggestions of things she did when she previously encountered a similar problem.

I especially want to thank my family for providing emotional support as well as encouraging me to keep going even when it was difficult.

I want to thank the University of California, Irvine for providing me with the opportunity to deepen my knowledge of physics and astronomy, as well as build an appreciation for the scientific process.

Financial support was provided by the University of California, Irvine and NSF grant AST-1412693.

ABSTRACT OF THE THESIS

JAVELIN Analysis of the Lick AGN Monitoring Project 2011

By

Andrew Peter Brandel

Master of Science in Physics

University of California, Irvine, 2017

Professor Aaron Barth

In 2011 Lick Observatory carried out a 2.5 month reverberation mapping campaign using the 3 meter Shane telescope monitoring 15 low redshift galaxies. The goal was to determine the black hole mass for each of these galaxies. My job was to use the JAVELIN software package to determine the size of the Broad Line Region around each of these objects and compare the results to those calculated using other methods. Here I present my findings for the 6 targets that JAVELIN found lag times for at least one of the emission lines. I also include the results using CCF which are in the process of being published.

INTRODUCTION

It is now widely believed that most if not all massive galaxies contain a central supermassive black hole. Determining the mass of these central black holes is an important area of research in astrophysics. Knowing the mass of the central black hole for a broad range in redshift of host galaxies over provides information about galactic evolution. It is particularly useful for studying feedback between accretion and star formation, and growth of black holes within different host galaxy environments. If the central black hole is accreting material it is classified as an Active Galactic Nucleus, or AGN.

The morphology of an AGN has several key features; the central black hole, the accretion disk, the Broad Line Region, the Narrow Line Region, a relativistic jet, and an obscuring torus. The most useful feature for reverberation mapping is the Broad Line Region (BLR). The BLR is composed of gas orbiting close to the black hole at high speeds while being ionized by the continuum radiation. The accretion of material into the AGN is a chaotic process so the luminosity of the AGN varies over time. To measure this, images are taken of the galaxy over a period of time, the duration of which depends on the mass. The total flux from all the stars in the galaxy will not change over the course of several weeks so any variation in the overall flux must come from the central AGN. The variation in the AGN can be computed and a light curve of the continuum flux can be constructed.

The variability in the intensity of the flux from the continuum leads to an ionizing response in the BLR flux, so if the continuum increases in flux, so will the emission. It is generally accepted that the light curves follow the relationship

$$L(t) = \int_{-\infty}^{\infty} \Psi(\tau) C(t-\tau) d\tau \quad (1)$$

where L(t) is the emission line light curve, C(t) is the continuum light curve, and Ψ(t) is the "transfer function" that will depend on the geometry and dynamics of the system (White & Peterson 1994).

The ionizing photons from the continuum travel at the speed of light out to the BLR so by multiplying the time it takes for the BLR to respond to the continuum by the speed of light, the size of the BLR is calculated. This is the principle of reverberation mapping. This technique is useful because most AGNs are too far away to make accurate measurements of the gas and stellar dynamics, but by observing the AGN in the time domain they can be temporally resolved. To measure the emission line light curve, spectroscopic measurements are taken of the object over the same period as the continuum measurements. With data from both the continuum light and data from the emission lines in the BLR, a time difference can be calculated (Blandford & McKee 1982).

The gas in the BLR is orbiting around the central black hole with some unknown velocity. However, because this gas is orbiting, it will have a different line of sight velocity at each position around its orbit. Therefore, the emission lines will be blueshifted and redshifted on either side of its orbit. This is the principle of Doppler broadening. The more the emission lines are spread out, the faster the gas must be orbiting. Therefore, by measuring the width of the emission lines, the velocity dispersion of the gas can be calculated.

CHAPTER 1: Background on AGN

When observing black holes, it is useful to have an estimate of the mass of a given AGN before observing it. The expected lag result can be found using the Radius-Luminosity relationship (Bentz et al. 2013). This paper observed 41 AGNs ranging in luminosity of four orders of magnitude that had previously been studied and where Hβ lags had been determined. First a distance had to be known for each galaxy, which for most of them had to be determined by measuring the redshift due to the cosmic expansion. This adds some error into the calculation due to relative motion. Comparing the flux values and the distance to each object a luminosity was determined. A power law was then fit comparing the size of the BLR and the luminosity. The result was consistent with a simple photoionization model across multiple orders of magnitude in luminosity. Thus, if an AGN is observed with a given luminosity, an expected lag value can be determined that follows this relationship. This also allows the AGN to potentially be used as a standard candle. Once the BLR size is known and the apparent luminosity is measured a distance can be calculated.

To get accurate measurements of the AGN, measurements need to be sampled several times longer than the expected lag result. For example, if the lag was seven days long, data would need to be taken over a span much longer than seven days to compute a statistically significant result. Therefore, both the AGN continuum and the BLR emission lines must be measured over several months to accurately line up the two light curves with a lagged separation. The temporal response of the emission light curve to the continuum light curve can then be computed. This gives a spatial size to the broad line region.

However, the BLR is not just at a single location, it is spread out over several light days so measurements are taken for multiple emission lines, corresponding to multiple radii, to determine the overall size of the BLR. Emission lines corresponding to high ionization energy are located close to the central engine, while lines with low ionization energy are further out. The emission lines from the continuum radiation originate near the black hole where the gas is orbiting quite fast, typically hundreds of kilometers per second. Due to this fast rotation, the emission lines undergo Doppler broadening. The width of this line can be measured. Combining measurements of the BLR size with velocity measurements allows for an estimate of the virial mass of the black hole using a standard Newtonian potential

$$M_{BH} = f\frac{c\tau(\Delta v)^2}{G} \tag{2}$$

where τ is the time lag, Δv is the emission line broadening due to the Doppler effect, cτ is the size of the BLR, and G is the gravitational constant (Peterson et al. 2004).

However it is complicated by other dynamics of the BLR, such as inflow and outflow, geometry etc. which change the scaling factor f. Thus, what is sometimes done is a calculation of the virial product ($\frac{c\tau(\Delta v)^2}{G}$) and fit a value for f that satisfies the $M_{BH} - \sigma_*$ relation (Onken et al. 2004). In summary this paper operated under the assumption that the velocity dispersion, not the FWHM of the emission line, is a better measurement of Δv, then applying f scaling factors corresponding to the two different best fits for quiescent galaxies to the AGN, a central black hole mass was determined for 16 different AGNs. It was further constrained that the $M_{BH} - \sigma_*$ relation present in quiescent galaxies is consistent for AGN as well. It is not required to make any assumptions about the geometry and use these average values for f to determine black hole mass.

Recently there have been efforts to better determine what the scaling factor is for a given galaxy thus providing a more precise value for the black hole mass. The code CARAMEL (Pancoast et al. 2011) aims to do this by modeling the BLR with different combinations of geometric structures such as disks, shells, tori as well as including inflowing and outflowing of gas. This is then observed at different angles. This model can then be used as a template that actual continuum light curve data can be propagate through. This produces modeled emission light curve data. Then comparing the actual emission data to the simulated data, the actual parameters of the BLR and black hole can be determined. This is useful because it gives another measurement of the black hole mass in addition to the $M_{BH} - \sigma_*$ relation, without making assumptions on the scale factor f.

Velocity dispersions are determined by fitting broadened stellar templates to the AGN spectra obtained (Barth et al. 2002). A stellar template is broadened and then fitted to the data, then a linear continuum is added to simulate the AGN continuum. This is then multiplied by a polynomial to account for systematic differences between the model and the actual data. This is repeated for several stellar types having different model spectra. This procedure gives a best fit for the velocity dispersion of the stellar bulge.

CHAPTER 2: LAMP 2011

The LAMP 2011 project was a reverberation mapping campaign to monitor 15 AGNs. This project focused on low luminosity, low mass AGNs with Hβ lags between about 4 to 12 days. These lag measurements were found using the interpolation cross-correlation function methods developed in previous works (White & Peterson 1994). Cross-correlation works by taking two different functions and calculates how well correlated they are for different values of lag. For example, if one function was sin(t) and the other was cos(t) the cross-correlation would yield a correlation at $\pi/2$. Real data does not have perfect sampling, so there will be some spread in the correlation values calculated.

In the context of reverberation mapping, the first function is the continuum light curve and the second is an emission light curve that is defined such that it is the same as the continuum light curve with a delay in the time domain. However, the light curves are not continuous functions but are made up of discrete points. Model light curves were made using the interpolation cross-correlation function method. This constructs a light curve by linearly interpolating adjacent points in the data (Gaskell & Peterson 1987). These light curves were then run through a series of IDL packages developed from previous reverberation mapping studies (Barth et al. 2011a). These input different fitting parameters for the two lines and builds up a probability distribution for different lag values that line up the two curves. Using this method, LAMP 2011 successfully determined the lags of 8 of the 15 sampled AGNs.

My job was to also run the light curves through a program called JAVELIN. This program was written by astronomers at Ohio State University to calculate lag times of light curves (Zu et al. 2011). It assumes that the emission light curve is scaled and smoothed version

of the continuum light curve. It models variation in the AGN continuum as a damped random walk with covariance function

$$S_{\Delta t} = \sigma^2 e^{-\left|\frac{\Delta t}{\tau_d}\right|} \quad (3)$$

where σ is the variability amplitude and τ_d is the exponential damping timescale. JAVELIN is also able to directly determine the uncertainty in its generated light curve and fit more than one emission line simultaneously. JAVELIN then assumes that the emission and continuum light curves are correlated and tries to determine a lag between the two. It does this by fitting σ and τ_d for the continuum, then models the emission light curve as a response to the continuum. It does this by running several Markov Chain Monte Carlo Simulations. It then builds up a distribution of predicted lag values. The goal was to see if JAVELIN was more accurate or computationally efficient than the previous methods of cross-correlation fitting. My job was to run this program with various input parameters and see what kind of results could be obtained.

The first thing I did was prepare the data to be fed into JAVELIN. To begin, I had to give corrections to the errors listed in the light curve files. It is assumed that the [O III] line flux does not change over the observing campaign. Any observed variation in the measured [O III] line must be due to a residual flux calibration error. This additional scatter was added into the error budget for the data. This was done by multiplying the average continuum flux counts by the [O III] scatter, and adding in quadrature to the given uncertainties for each data point in the continuum light curve.

JAVELIN also has issues matching up light curves with vastly different flux values. While JAVELIN does assume that the emission line is scaled version of the continuum, it does have limits on how much it can scale. The continuum light curves typically had fluxes an order

of magnitude higher than the emission fluxes, so I had to scale the continuum to match these emission light curves. Because the Hβ line had the best signal to noise, and was measured for each object, I scaled each continuum line to the corresponding Hβ line. To achieve this I divided the standard deviation of the Hβ light curve by the standard deviation of the continuum light curve. I then multiplied the continuum light curve and corresponding error values by this ratio. Finally, I subtracted the mean of this scaled continuum from each data point to try to find a zero point, then added the mean value of the Hβ light curve to each data point to try to line them up to the same scale.

The next thing I had to do was figure out at what point having more computational time was not giving a more robust answer, ie where computation time had diminishing returns. After running through several tests, I finally settled on MCMC parameters of 100 starting walkers, a 1000 step chain, and a burn in time of 500. If a data set did not converge to a solution by this point, adding extra time was not helping to find one. After the parameters were set I compared the continuum light curve to each of the emission line light curves for each AGN. For most of the objects this was sufficient to converge on a calculated lag value. Some objects, however, had a large range in the lag values calculated. JAVELIN can compare more than 2 light curves at a time, thus being more robust in determining lag values. I then used the continuum light curve, a strong signal to noise light curve as an anchor, in our data sets Hβ was the best candidate, and a third light curve that had a large spread that I wanted to refine. This essentially gives the third light curve 2 curves to match up, the continuum and the Hβ emission line. Using this technique, I refined some of the noisier emission lines to produce lag values. Some of our objects only had Hβ emission data so I was only able to use this method on objects that had data for more than

one emission line. JAVELIN is also able to use 3 emission light curves, but these did not lead to any different results than only the 2, and led to large computational time so no lag values were

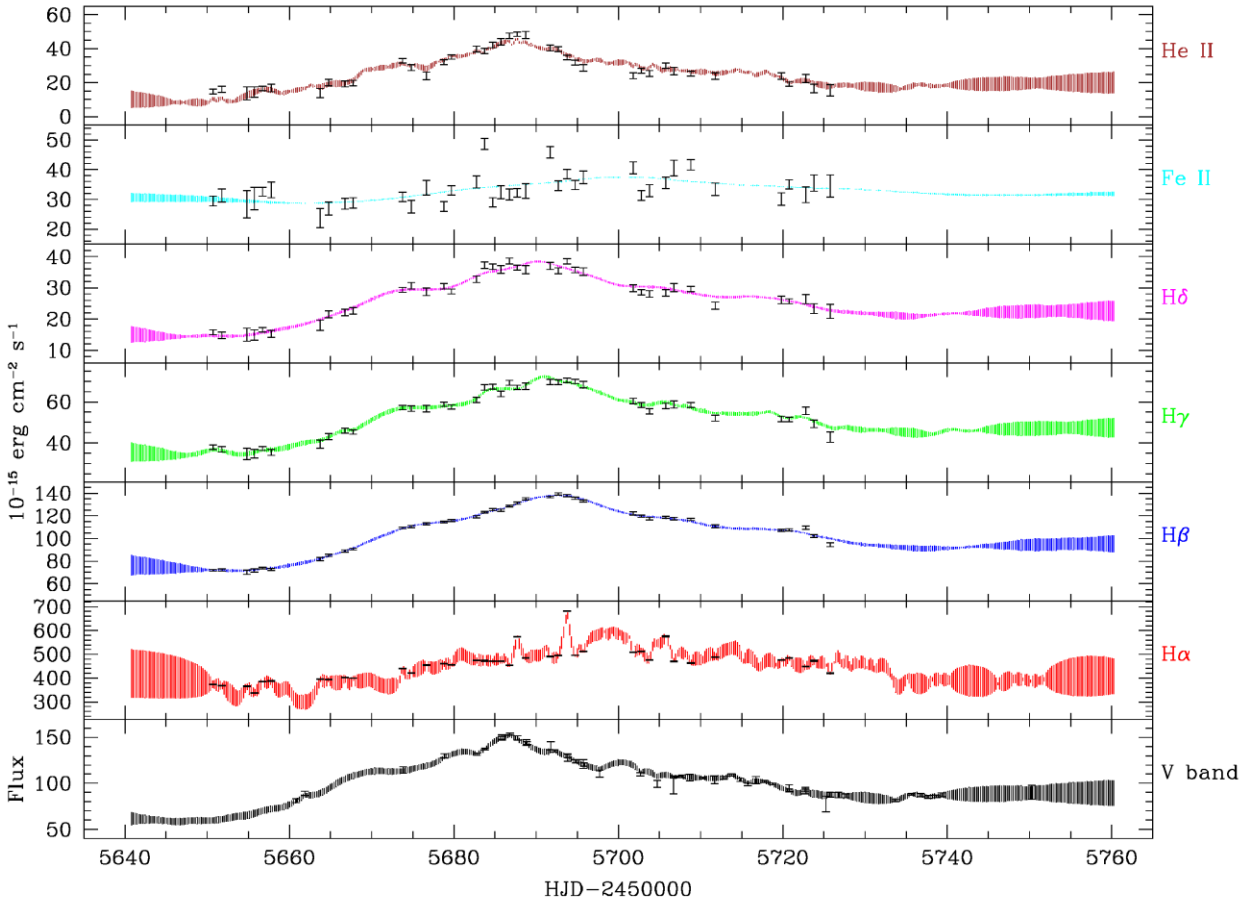

Figure 2.1. Light curve for Mrk 40. The data points and error bars represent the measurements for each of the emission lines and V band fluxes. The colored bands are the fitted light curves and associated errors calculated in JAVELIN for each line.

computed using 3 emission lines simultaneously. The calculated light curves for each object are shown in Figures 1-6, while the resulting lag distributions are shown in Figures 7-12.

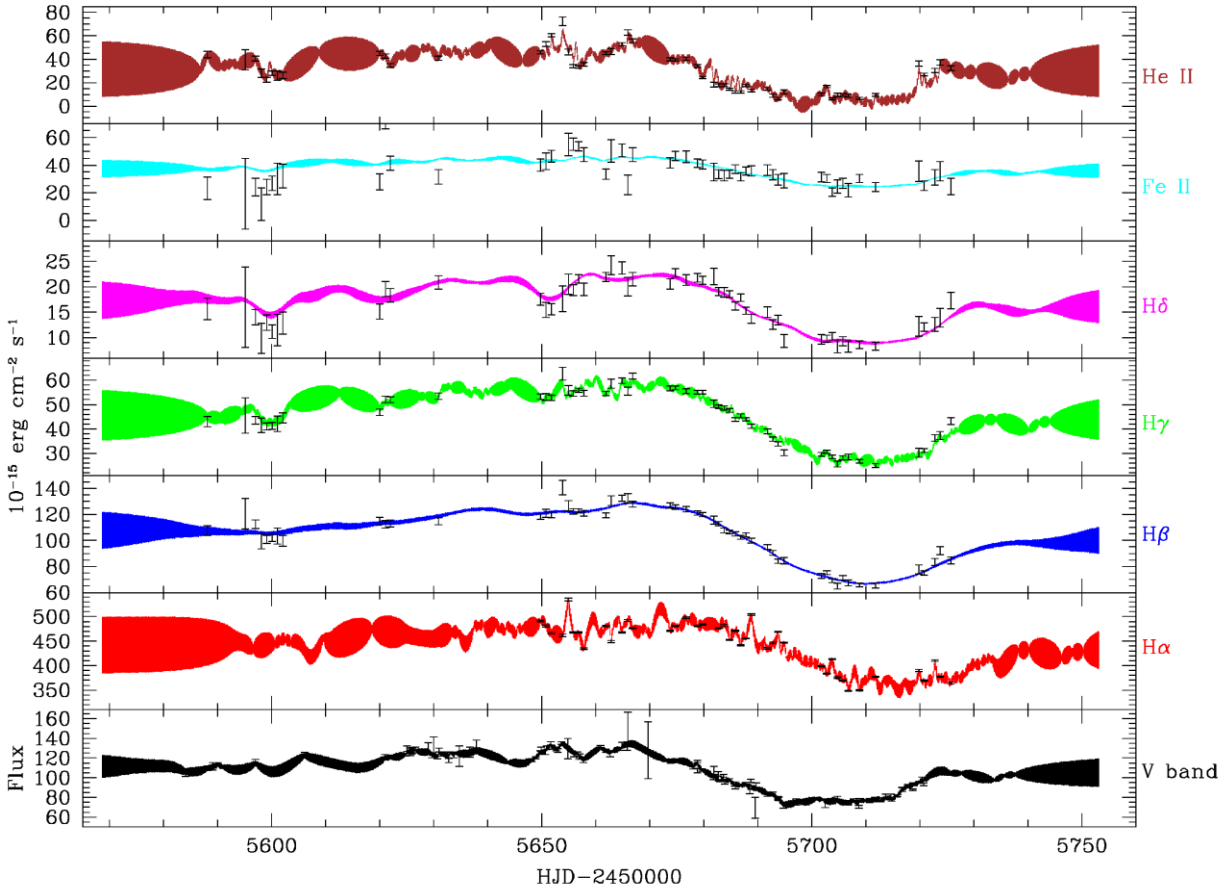

Figure 2.2. Light curve for Mrk 50

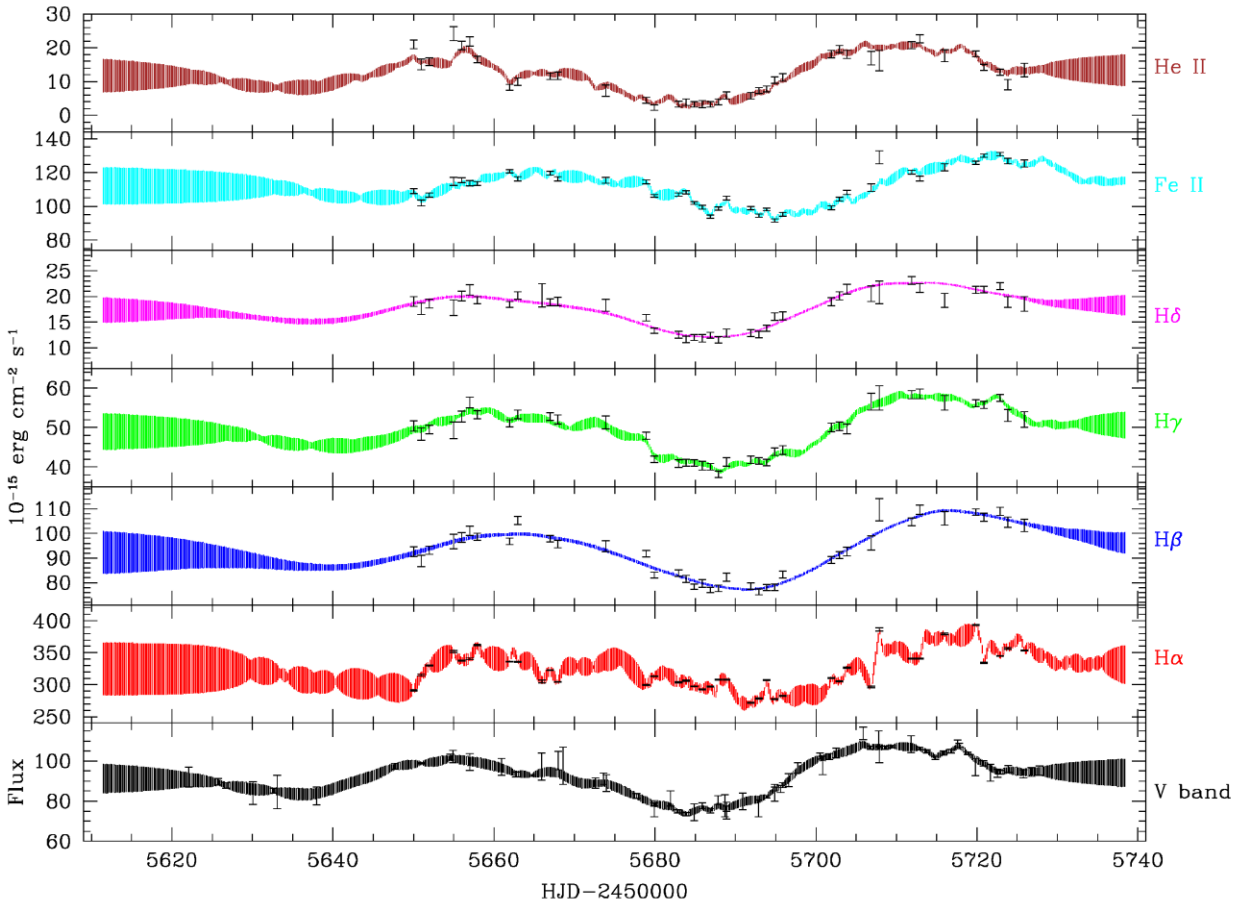

Figure 2.3. Light Curve for Mrk 1511

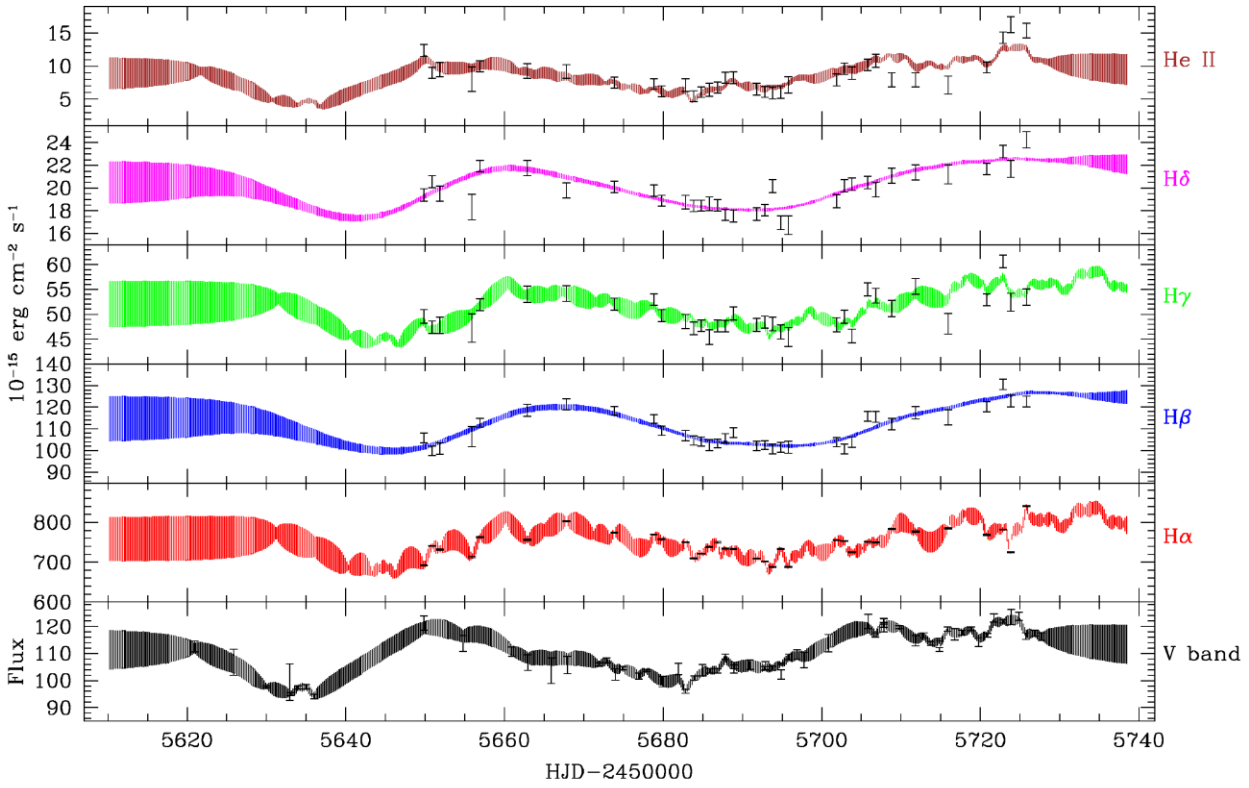

Figure 2.4. Light Curve for Mrk 279

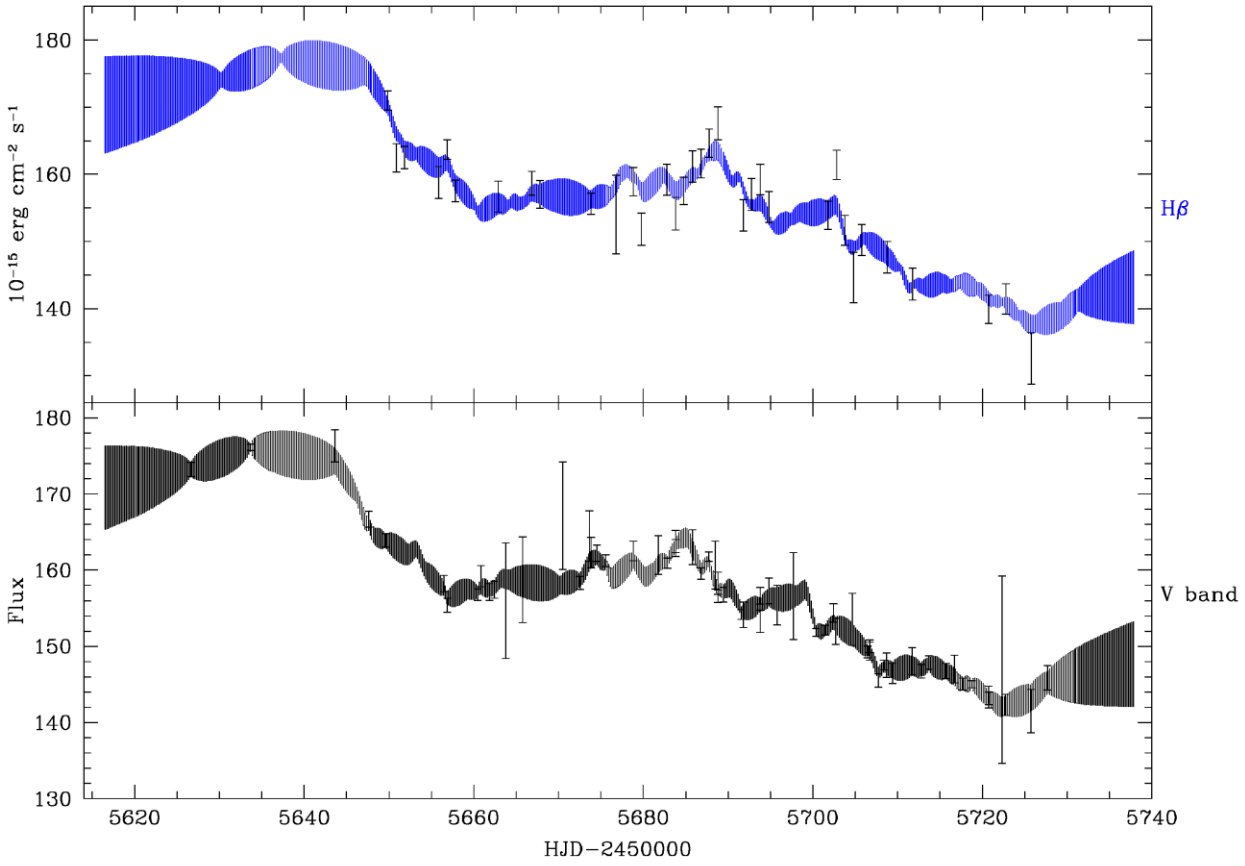

Figure 2.5. Light Curve for PG 1310

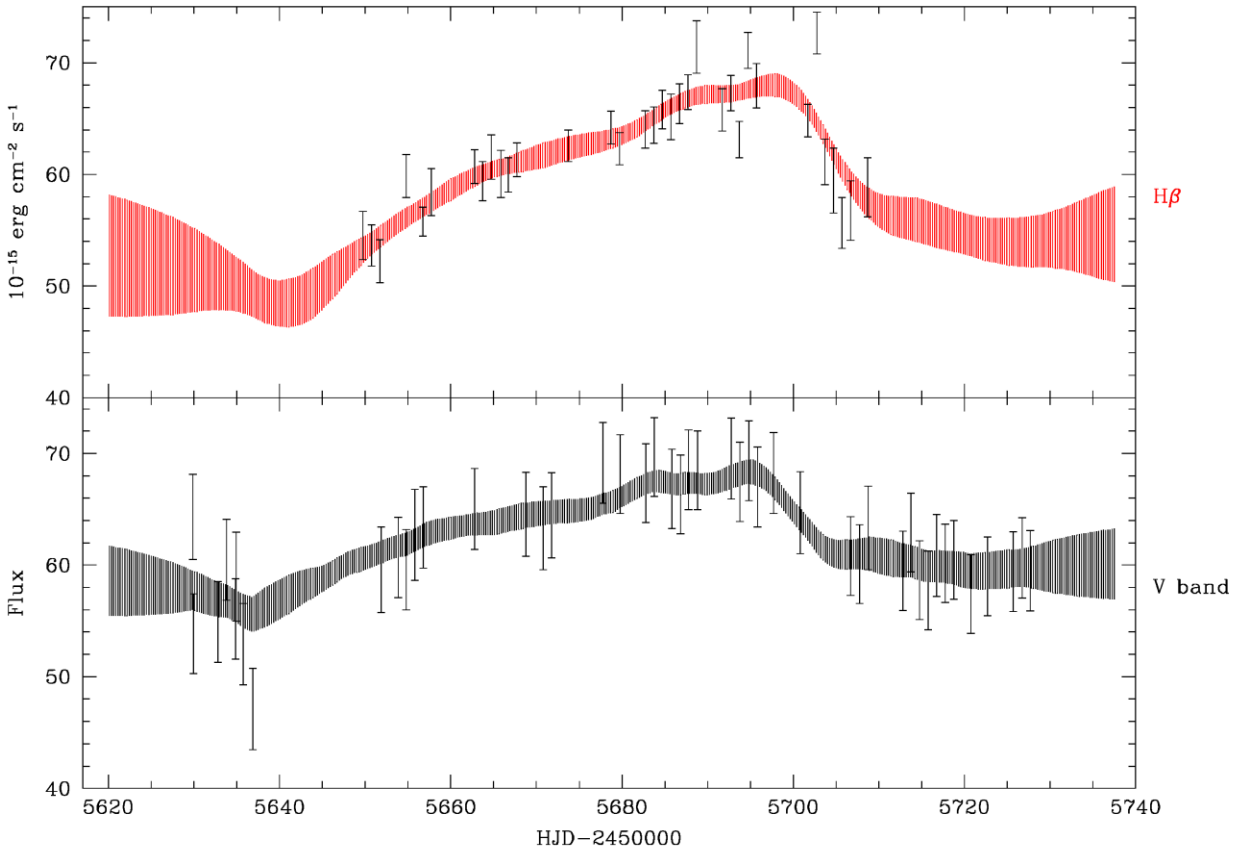

Figure 2.6. Light Curve of Mrk 141

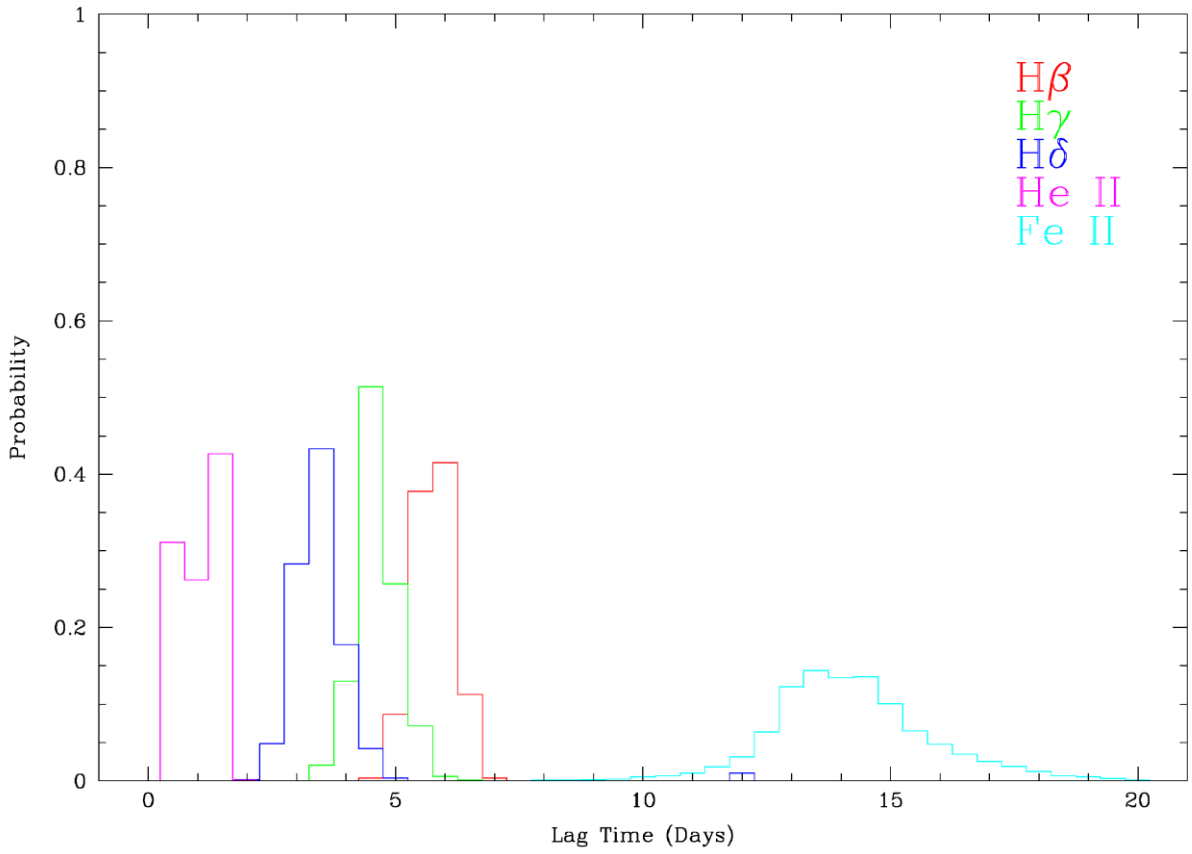

Figure 2.7. Lag Distribution for Mrk 40 binned in 0.5 day increments

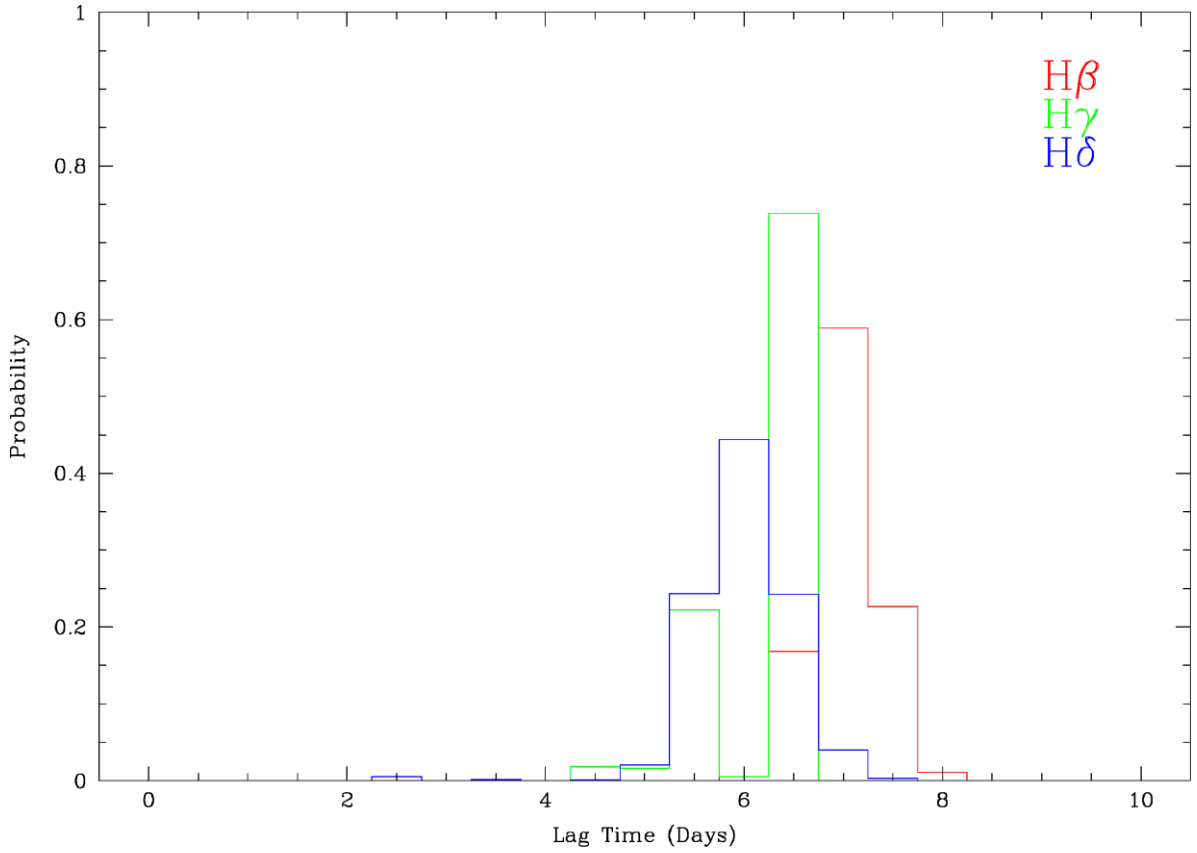

Figure 2.8. Lag Distribution for Mrk 50

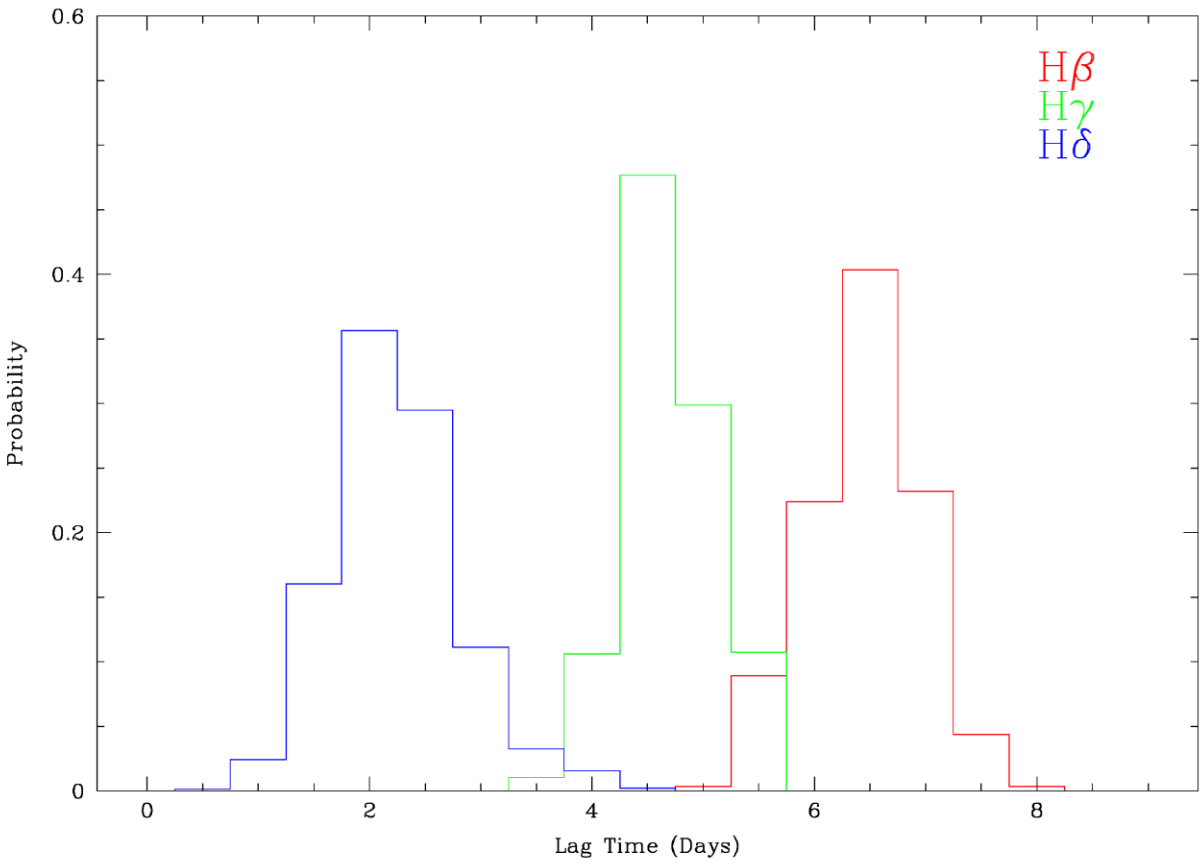

Figure 2.9. Lag Distribution for Mrk 1511

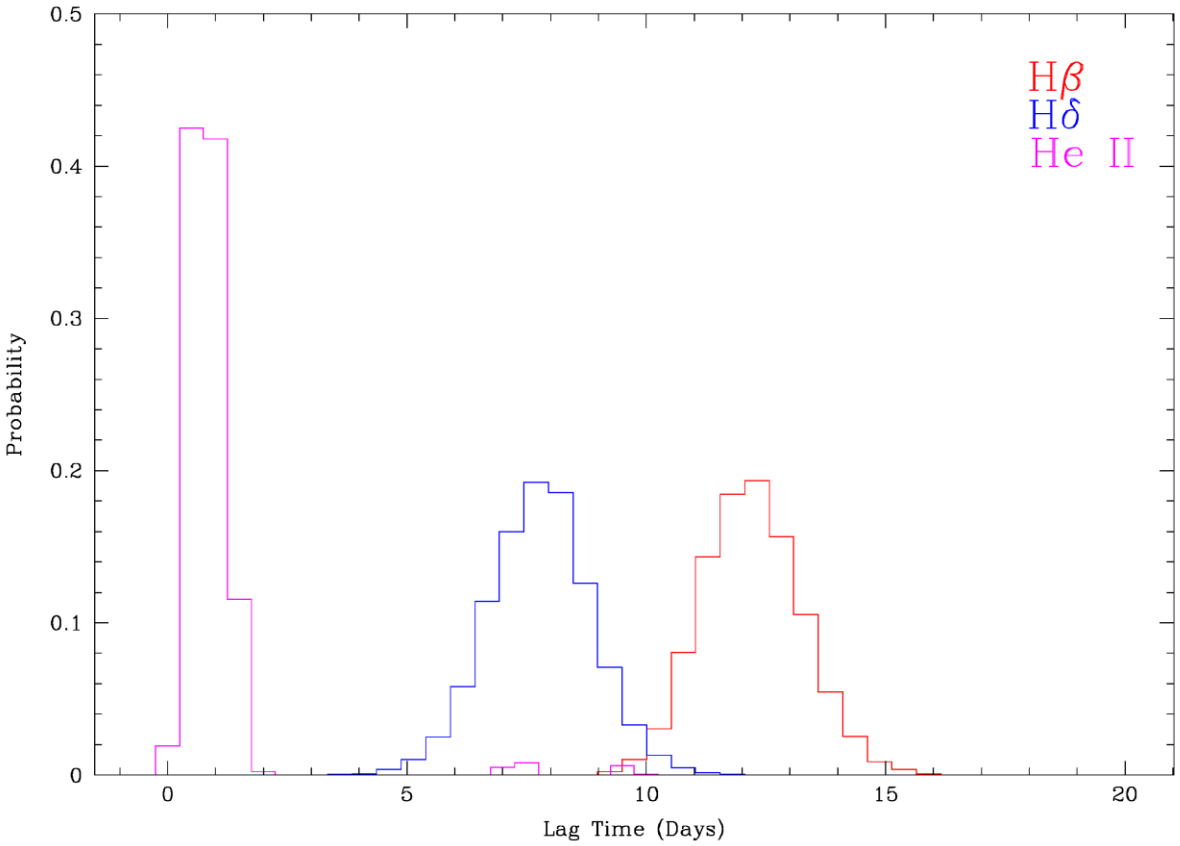

Figure 2.10. Lag Distribution for Mrk 279

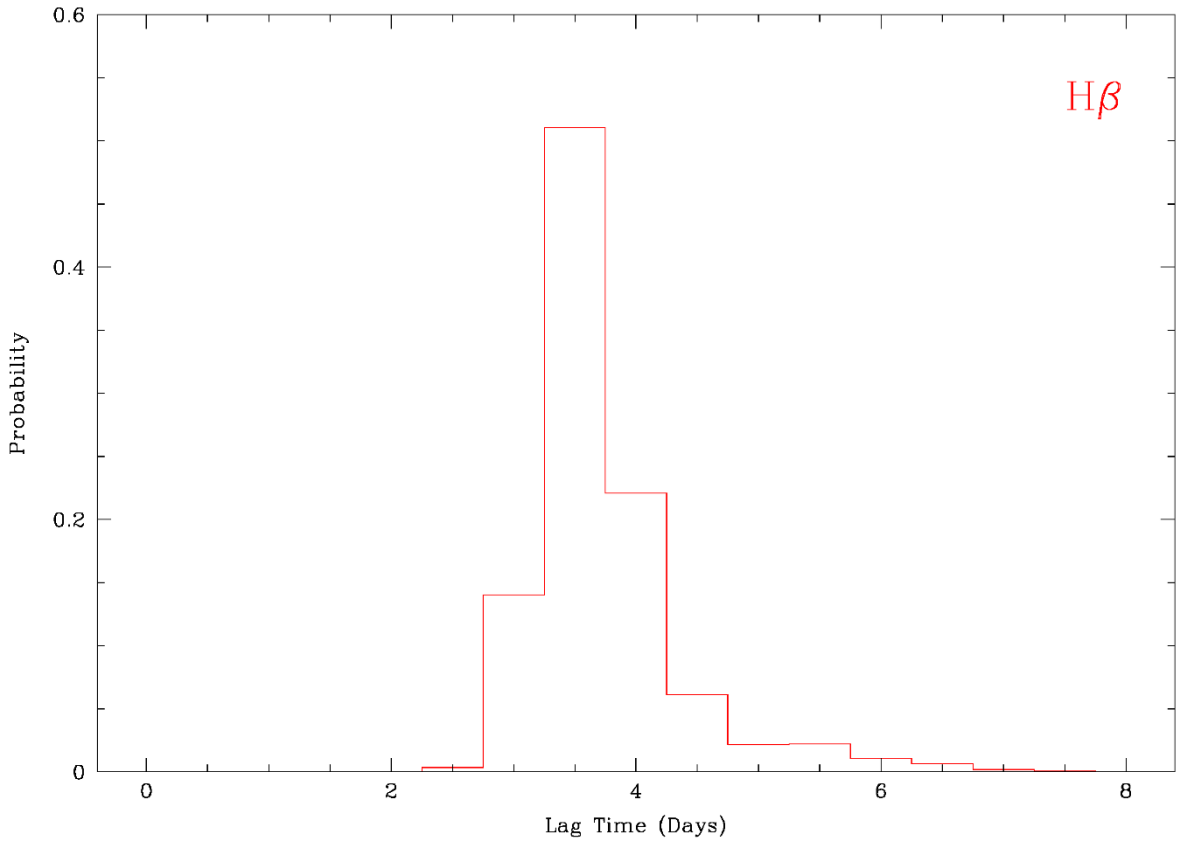

Figure 2.11. Lag Distribution for PG 1310

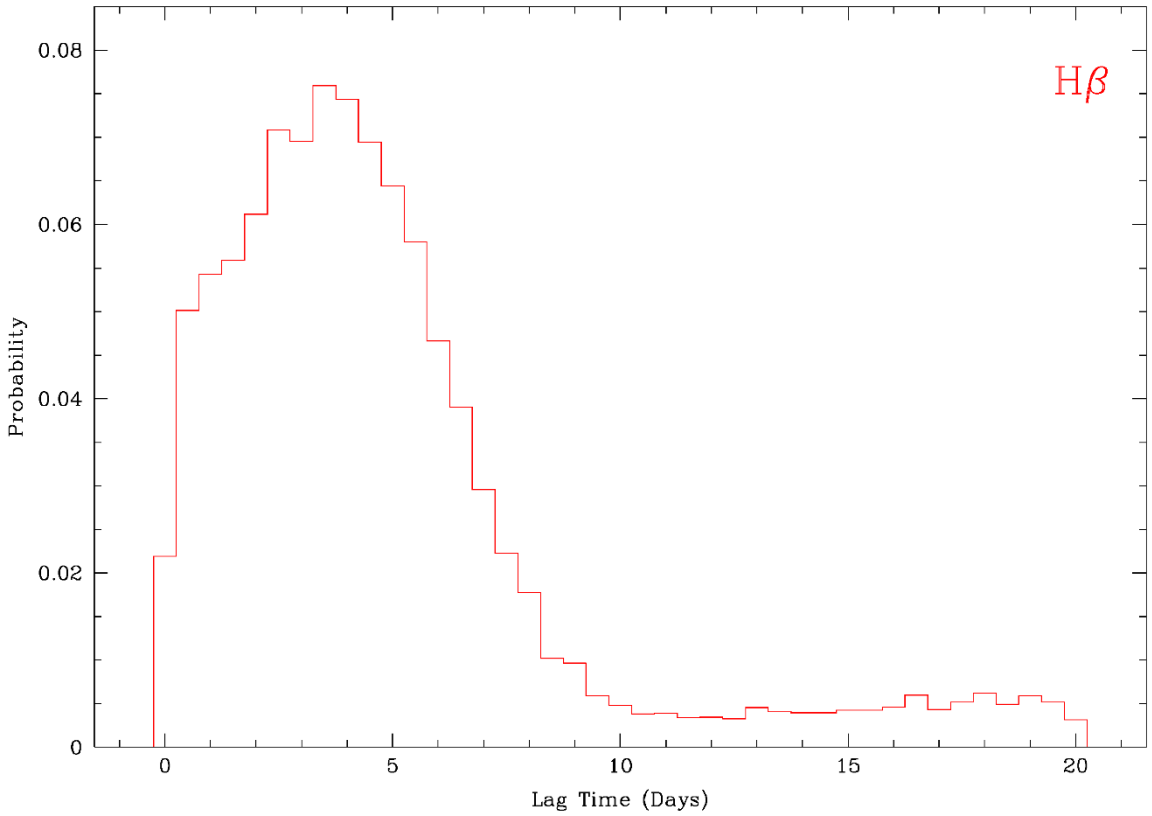

Figure 2.12. Lag Distribution for Mrk 141

There were several issues with running this program. First JAVELIN was sometimes not able to converge on a solution. This happened when the data had a low signal to noise ratio or was not well sampled. It also happened on AGNs that did not have much variability. This led to JAVELIN trying too hard to fit the data. For example, when the error bars on each data point are small compared to the variability, JAVELIN tries to match the light curve to these precise points. This leads to a nonsensical result of high variability. Figure 13 shows an example of this. One way to solve this is to increase the size of the error bars. I did this by multiplying the errors calculated by increasing integer values until the high variability signal was removed in the fitting

process. This either did not give a more reasonable answer, or the error needed to be increased so much that the resulting light curve would not show variability.

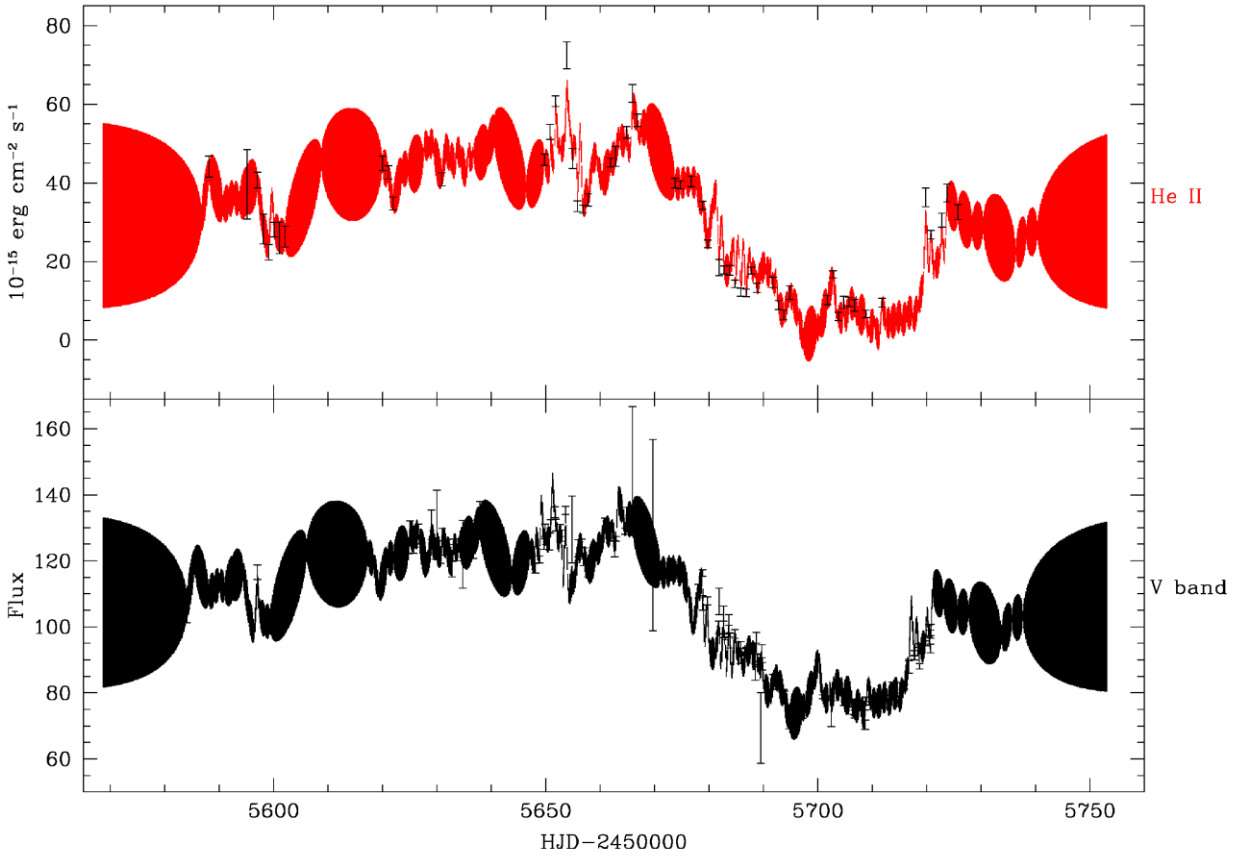

Figure 2.13. Mrk 50 is an example where JAVELIN tried too hard to fit high variability to He II

A more robust way is having JAVELIN ignore variability less than some specified time, chosen to be 0.75 days. Even after all of these corrections, JAVELIN can still fail to converge on a single solution and give multi-peaked solutions. This happened for 8 AGNs due to poor sampling or noisy data. LAMP 2011 successfully determined virial mass measurements for 8 AGNs as well tighter constraints on the $M_{BH} - \sigma_*$ and BLR radius-luminosity relations using CCF. Using JAVELIN, I determined lag measurements for at least Hβ, that could then be used to determine virial masses, for 6 AGNs. The results I found were in reasonable agreement with

those found through CCF. Table 2.1 shows the results from JAVELIN and compares to those found using CCF. Black hole mass was computed using f=5.9 (Woo 2013). These results for both CCF and mine from JAVELIN are in the process of publication.

Table 2.1. Line Widths, Lags from CCF and JAVELIN, and Black Hole Mass

Object	Emission Line	$\tau_{JAVELIN}$	τ_{cen}	τ_{peak}	$\sigma_{H\beta}$(km s^{-1})	$M_{BH}(10^6 M_\odot)$
Mrk 40	Hα	-	$7.97^{2.65}_{-2.20}$	$8.00^{3.50}_{-1.50}$		
	Hβ	$5.78^{0.39}_{-0.40}$	$5.61^{0.66}_{-0.84}$	$5.50^{1.25}_{-1.00}$	740 ± 17	$3.63^{0.42}_{-0.40}$
	Hγ	$5.22^{0.66}_{-0.74}$	$3.97^{0.81}_{-0.78}$	$4.75^{1.00}_{-1.00}$		
	Hδ	$3.28^{0.54}_{-0.47}$	$2.77^{0.76}_{-0.78}$	$3.50^{1.25}_{-1.75}$		
	He II	$0.40^{0.24}_{-0.22}$	$0.28^{0.65}_{-0.65}$	$0.00^{0.75}_{-0.50}$		
	Fe II	$12.61^{0.98}_{-0.55}$	$11.35^{4.29}_{-2.76}$	$1.00^{3.75}_{-2.75}$		
Mrk 50	Hα	$15.36^{1.25}_{-2.91}$	$15.80^{2.10}_{-2.11}$	$14.50^{2.00}_{-2.75}$		
	Hβ	$7.03^{0.31}_{-0.66}$	$8.66^{1.63}_{-1.51}$	$6.50^{2.25}_{-1.50}$	2020 ± 103	$32.88^{5.04}_{-6.05}$
	Hγ	$5.50^{0.08}_{-0.10}$	$7.82^{1.49}_{-1.43}$	$5.75^{1.25}_{-1.00}$		
	Hδ	$6.21^{0.43}_{-0.43}$	$9.55^{1.81}_{-1.68}$	$8.00^{1.75}_{-2.50}$		
	He II	$2.65^{0.39}_{-0.40}$	$-2.60^{1.16}_{-1.00}$	$-0.75^{0.75}_{-1.00}$		
	Fe II	$13.11^{3.72}_{-1.05}$	$8.69^{4.04}_{-3.35}$	$11.00^{3.50}_{-8.50}$		
Mrk 141	Hβ	$4.01^{3.23}_{-2.47}$	$5.63^{8.27}_{-1.65}$	$5.50^{9.00}_{-1.75}$		
Mrk 279	Hα	$9.57^{0.81}_{-0.10}$	$11.84^{3.90}_{-2.31}$	$12.50^{4.50}_{-3.00}$		
	Hβ	$12.38^{1.03}_{-1.24}$	$13.88^{1.55}_{-2.76}$	$14.25^{2.75}_{-4.25}$	1778 ± 71	$44.87^{7.69}_{-7.65}$
	Hγ	$11.48^{1.28}_{-1.13}$	$13.01^{3.77}_{-6.61}$	$12.25^{5.25}_{-5.50}$		
	Hδ	$8.84^{1.12}_{-1.09}$	$6.11^{2.86}_{-3.31}$	$6.50^{5.00}_{-2.75}$		
	He II	$1.53^{5.73}_{-0.85}$	$0.74^{4.09}_{-1.08}$	$0.75^{1.75}_{-1.50}$		
Mrk 1511	Hα	$7.67^{0.87}_{-0.08}$	$1.37^{1.15}_{-1.61}$	$3.25^{0.75}_{-1.75}$		
	Hβ	$6.48^{0.46}_{-0.52}$	$3.54^{0.76}_{-0.82}$	$2.50^{1.00}_{-0.75}$	1506 ± 42	$16.85^{2.22}_{-2.20}$
	Hγ	$4.52^{0.26}_{-0.35}$	$2.69^{0.95}_{-0.70}$	$1.75^{1.00}_{-0.25}$		
	Hδ	$2.01^{0.46}_{-0.46}$	$1.59^{0.65}_{-0.80}$	$1.25^{0.25}_{-0.25}$		
	He II	$0.20^{0.28}_{-0.15}$	$0.21^{0.89}_{-0.59}$	$-0.25^{0.50}_{-0.25}$		
	Fe II	$10.63^{0.13}_{-0.13}$	$6.64^{1.24}_{-1.29}$	$5.50^{1.25}_{-1.00}$		
PG 1310	Hβ	$3.61^{0.47}_{-0.34}$	$7.20^{2.41}_{-3.11}$	$4.75^{7.75}_{-1.50}$		

CONCLUSION

Several universities are contributing to LAMP 2016, a follow up to LAMP 2011. This aims to probe higher luminosity AGNs to determine the size of the BLR. Because they have higher luminosity, they will have larger BLR, and therefore larger lag times, so must be observed over a longer duration. The AGNs being observed have expected Hβ lag values in the 20-60 day range, significantly longer than previous studies. Due to the large lag values, the campaign was scheduled to last 8 months (April 2016 to January 2017) to ensure the targets are observed several times longer than the lag values. The data collected during the early parts of the campaign allowed for an extension through May 2017. I am a part of this collaboration, helping to observe each of the targets from the UCI remote observing room. Once the campaign has finished and the data has been reduced, it will need to be analyzed. By using JAVELIN as well as other methods stated previously, AGN dynamics and properties can be studied. Lag times will be computed for new targets, as well as constrain ones previously studied. Combining these with velocity measurements and models of geometry, central black hole virial masses can be computed.

REFERENCES

Barth, A.J., Bennert, V.N., Canalizo, G., et al. 2015, ApJ, 217, 26

Barth, A.J., Ho, L.C., Sargent, W.L.W. 2002, ApJ, 124, 2607

Barth, A.J., Nguyen, M.L., Malkan, M.A., et al. 2011a, ApJ, 732, 121

Bentz, M.C., Denney, K.D., Grier, C.J., et al. 2013, ApJ, 767, 149

Blandford, R.D., McKee, C.F. 1982, ApJ, 255, 419

Gaskell, C.M., Peterson, B.M. 1987, ApJ, 65, 1

Grier, C.J., Martini, P., Watson, L.C., et al. 2013b, ApJ, 773, 90

Kaspi, S., Smith, P.S., Netzer, H., et al. 1999, ApJ, 533, 631

Metzroth, K.G., Onken, C.A., Peterson, B.M. 2006, ApJ, 647, 901

Onken, C.A., Ferrarese, L., Merritt, D., et al. 2004, ApJ, 615, 645

Pancoast, A., Brewer, B.J., Treu, T. 2011, ApJ, 730, 139

Park, D., Kelly, B.C., Woo, J.H., et al. 2012, ApJ, 203, 6

Pei, L., Barth, A.J., Aldering, G.S., et al. 2014, ApJ, 795, 38

Peterson, B.M., Ferrarese, L., Gilbert K.M., et al. 2004, ApJ, 613, 682

Tremaine, S., Gebhardt, K., Bender, R., et al. 2002, ApJ, 574, 740

White, R.J., Peterson, B.M. 1994, ApJ, 613, 682

Woo, J.H., Schulze, A., Park, D., et al. 2013, ApJ. 772, 49

Zu, Y., Kochanek, C.S., Peterson, B.M. 2011, ApJ, 735, 80